Monolayer Ice

Ronen Zangi* and Alan E. Mark

Department of Biophysical Chemistry, GBB, University of Groningen, Nijenborgh 4, 9747 AG Groningen, The Netherlands

(Received 4 October 2002; published 8 July 2003)

We report results from molecular dynamics simulations of water under confinement and at ambient conditions that predict a first-order freezing transition from a monolayer of liquid water to a monolayer of ice induced by increasing the distance between the confining parallel plates. Since a slab geometry is incompatible with a tetrahedral arrangement of the sp^3 hybridized oxygen of water, the freezing is coupled to a linear buckling transition. By exploiting the ordered out-of-plane displacement of the molecules in the buckled phase the distortion of the hydrogen bonds is minimized.

DOI: 10.1103/PhysRevLett.91.025502 PACS numbers: 61.20.Ja, 61.46.+w, 68.15.+e

Bulk ice exhibits a rich polymorphism of phases that are built of tetrahedrally coordinated hydrogen-bonded water molecules [1]. While in ordinary ice the tetrahedral geometry is nearly perfect, in most other ice phases distortions from ideal geometry occur. This involves bending of the hydrogen bonds at the expense of bond strength. Hydrogen bonding interactions are insufficient to initiate the rehybridization of the sp^3 hybridized oxygen atom and thus a change in either the molecular H-O-H angle or in the spatial distribution of the electron lone pairs. In principle, the tetrahedral arrangement of water is incompatible with a two-dimensional geometry. Nevertheless, under confinement a competing phenomenon comes into play. In general, confinement of a liquid to a film thinner than 4–6 molecular layers will promote solidification. This is because the characteristic transverse density profile of a thin film can induce lateral ordering and result in freezing. The effect is stronger, as evidenced by an increase in crystalline elastic properties, as the space in which the system is constrained is reduced [2–4]. However, in experimental studies involving a mercury/water/mercury tunnel junction (weak wall-water interactions) at $T = 265$ K it was found that the Young's modulus of two-dimensional ice shows a maximum value (of $\sim$20% of bulk ice I_h) around a junction separation of 0.58 nm. This discontinuity in the elastic modulus raised the possibility of confinement-driven order-disorder phase transitions occurring as a function of film thickness [5].

In this study we utilize molecular dynamics (MD) simulation techniques to investigate the freezing of a water monolayer. Questions addressed include the following: What is the symmetry of a quasi-two-dimensional ice? What is the origin of the anomalous behavior observed for the Young's modulus of a quasi-two-dimensional ice? What is the nature of the melting/freezing transition of this system? Can water support buckled phases that so far have been observed only in colloidal suspension?

The simulations were performed using GROMACS 3.0 [6]. The five-site, tetrahedrally coordinated, TIP5P model [7] was used to describe the water molecules. A system of 780 water molecules was placed between two walls with a triangular arrangement of atoms out-of-registry with respect to one another. The water-wall interactions were represented by a 6–12 Lennard-Jones (LJ) potential with the parameters: $\sigma_{(O_w-W)} = 0.316$, $\sigma_{(H_w-W)} = 0.284$ nm and $\epsilon_{(O_w-W)} = 0.831$, $\epsilon_{(H_w-W)} = 0.415$ kJ/mol. These parameters represent approximately the van der Waals (vdW) interaction between a water molecule and a quartz (SiO_2) surface. The evaluation of the nonbonded interactions was performed using a twin range cutoff of 0.9 and 1.4 nm. To account for the neglect of electrostatic interactions beyond the long range cutoff a reaction-field correction assuming a relative dielectric of 78.0 was applied. Other simulation methodology used was the same as described previously [8].

A first set of simulations was run at constant plate separation, H, with $T = 300$ K and lateral pressure, P_l, coupling. The initial configuration was prepared by taking a thin layer ($H = 0.41$ nm) of water from a bulk configuration of the liquid and equilibrating for 30 ns. At each thermodynamic point (achieved by a sequential increase in H) the system was equilibrated for at least 15 ns and data collected for an additional 5 ns. Figure 1(a) shows the lateral diffusion coefficient for plate separations in the range $0.41\ \text{nm} \leq H \leq 0.59$ nm for lateral pressures of 1 and 100 bar. No obvious difference in the behavior of the system was evident for the two different lateral pressures. For plate separations in the range $0.41\ \text{nm} \leq H \leq 0.50$ nm the monolayer is liquid as indicated by the large diffusion coefficient and by the fact that the mean square displacement grows linearly with time [Fig. 1(b)]. At $H = 0.51$ nm the water molecules of the monolayer transform to a frozen state as indicated by a drop of 3–4 orders of magnitude in the lateral diffusion coefficient. In this state the dynamics of the molecules is best described in terms of small amplitude fluctuations around fixed positions with occasional cooperative jumps rather than as free diffusion [Fig. 1(c)]. Note, the MSD is not linear in the solid phase. Thus the determination of the diffusion coefficient from the slope of the MSD plot is

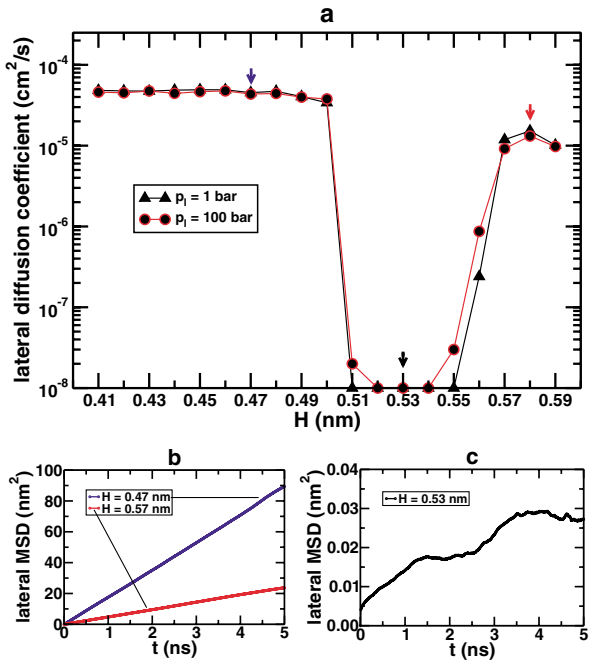

FIG. 1 (color online). (a) Inplane diffusion coefficients as a function of the distance between the confining parallel plates at $T = 300$ K. (b) Inplane mean square displacement as a function of time in the simulations with lateral pressure coupling of 1 bar for a monolayer and a bilayer of liquid water. (c) Lateral MSD as a function of time for a frozen water monolayer.

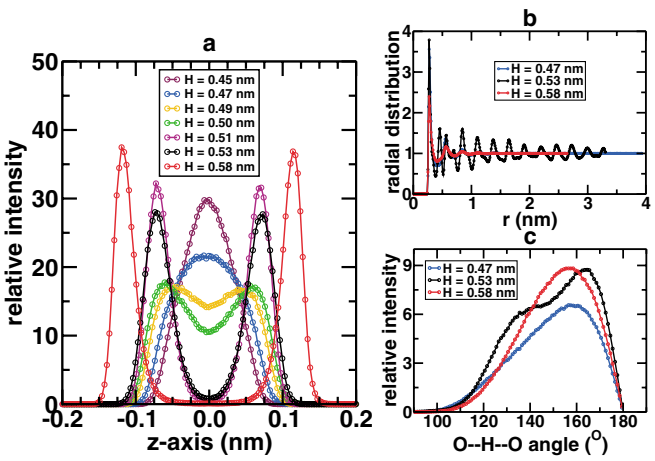

FIG. 2 (color). (a) Transverse distribution of the density of oxygen atoms for different plate separations, H. (b) Oxygen-oxygen radial distribution function. Most of the curve at $H = 0.47$ nm is hidden due to overlap with the distribution at $H = 0.58$ nm. (c) Hydrogen bond angle distribution. The ratio of the area under each plot corresponds to the ratio of the average number of hydrogen bonds per molecule, namely, 2.8:3.8:3.5 for $H = 0.47$, 0.53, 0.58 nm, respectively.

not strictly appropriate. However, the values obtained from such a procedure, shown in Fig. 1(a), provide a measure of the relative magnitude of the particles' displacement. At $H = 0.57$ nm the monolayer transforms into a bilayer of liquid water [see Fig. 2(a)]. The value of the lateral diffusion coefficient of liquid water in the monolayer is higher than in the bilayer due to the presence of interlayer hydrogen bonds in the bilayer resulting in an increase in connectivity and a decrease in mobility. Examination of the transverse density profile [Fig. 2(a)] reveals that the liquid state of the monolayer is characterized by a unimodal distribution. As H approaches the transition point ($H = 0.51$ nm), the distribution starts to develop two peaks adjacent to the walls. There is a clear bimodal character for $H \geq 0.51$ nm. The origin of this phenomenon is an excluded volume effect and is not due to a particular interaction between the molecules and the walls. The bimodal character of the normal density profile for $0.51\ \text{nm} \leq H \leq 0.56$ nm is due to a monolayer configuration which is buckled and only at $H = 0.57$ does the system transform to a bilayer where the normal density profile is also bimodal. The degree of spatial order of the oxygen atoms as indicated by the O–O radial distribution function for $H = 0.47$, 0.53, and 0.58 nm are shown in Fig. 2(b). The short range order in the plots corresponding to $H = 0.47$ and 0.58 nm reflect the disorder of the liquid phase. However, the long range order at $H = 0.53$ nm indicates that the system has the characteristics of an ordered crystalline phase. This freezing transition occurs at a temperature ($T = 300$ K) well above the freezing temperature of a bulk TIP5P water ($T < 270$ K) [9].

A transformation from a homogenous to a split normal density distribution of each layer in confined solids as a function of plate separation is a fingerprint of a buckling transition. Buckled phases were first observed in monolayers [10–13] and later in multilayers [14,15] of colloidal particles. The transition to a bimodal distribution of the transverse density is coupled to an inplane order-disorder transition. The lateral ordering takes the form of linear or zigzag rows of particles buckled against each other. The manifestation of the buckling transition enhances as the number of layers decreases.

Figure 3 shows a configuration after equilibration from a simulation of monolayer water ($H = 0.47$ nm), monolayer ice ($H = 0.53$ nm), and bilayer water ($H = 0.58$ nm). The ice monolayer has an inplane rhombic symmetry with respect to the positions of the oxygen atoms. The out-of-plane positions correspond to a linear buckled phase. Figure 2(c) shows that this out-of-plane displacement, together with the rhombic arrangement of the nearest neighbors, results in a hydrogen bond angle distribution with maxima at 164° and 139°. At the same time it allows each water molecule to be involved in four hydrogen bonds (in the liquid phase the unimodal distribution has a maximum at 159° for the monolayer and at 157° for the bilayer). Each water molecule donates to and accepts from its nearest neighbors present in the other vertical plane one hydrogen bond (this corresponds to the lower degree of the hydrogen bond bending, the peak at

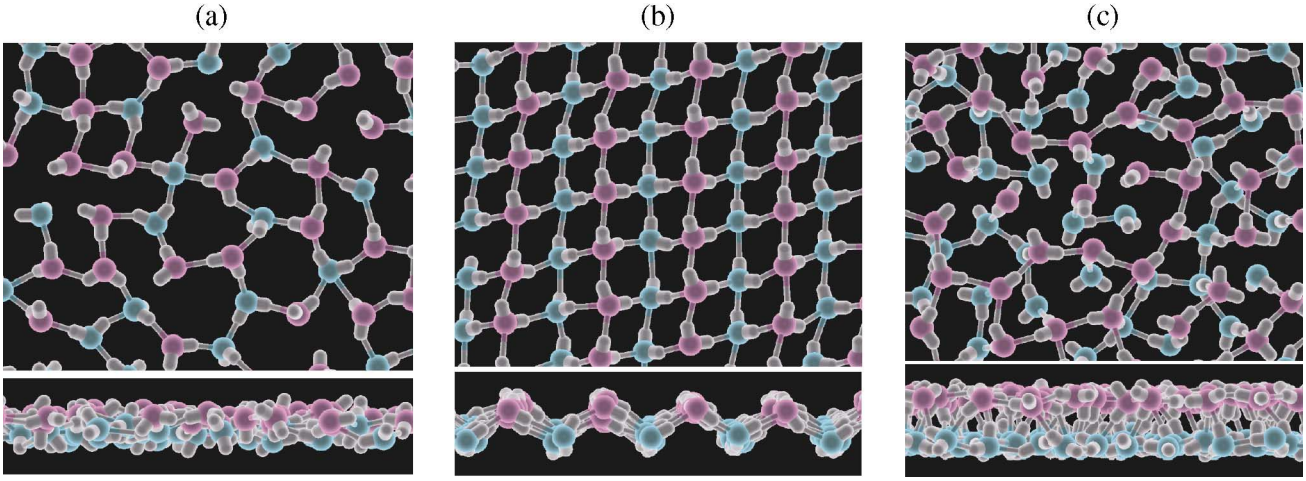

FIG. 3 (color). Snapshots from the MD simulations. Lateral and transverse views of (a) a water monolayer, $H = 0.47$ nm, (b) an ice monolayer, $H = 0.53$ nm, and (c) a water bilayer, $H = 0.58$ nm. Hydrogens are depicted in white. Oxygen atoms that lie above and below the midplane along the normal axis are depicted in magenta and cyan, respectively. Note, the phases are homogenous and the same degree of ordering is present throughout the entire box.

164°). In addition each water molecule donates to and accepts from its nearest neighbors present in the same vertical plane one hydrogen bond (this corresponds to the higher degree of the hydrogen bond bending, the peak at 139°). Following the treatment proposed by Pauling to estimate the residual entropy of ice I_h [16], the above connectivity pattern allows only two equivalent orientations of the water molecule with respect to its nearest neighbors (instead of six for ice I_h). However, since the probability that a given orientation of the central water is permitted by the orientations of the neighboring molecules is only 1/4, the total number of configurations for N molecules is $W = (2/4)^N$. Thus, there is no residual entropy, $S_0 = k_B \ln(W)$, arising from the disorder in the hydrogen positions, characterizing ice I_h. Therefore, the hydrogen positions must be ordered as is evident in Fig. 3(b). The density of the ice monolayer is in the range 0.90–0.91 g/ml. This is higher than the density of the water monolayer (0.79–0.87 g/ml) but lower than the density of the bilayer water examined in this study (1.11–1.16 g/ml).

The abrupt change in the dynamics and in the range of structural ordering during the freezing process suggests that the transition is first order. Simulations with temperature and lateral pressure coupling are the most appropriate to mimic experimental studies of confined system in mechanical equilibrium with the bulk, they do not allow, however, the simulation of phase coexistence. Determining the order of the transition in the present study is necessary since the nature of the melting transition in two-dimensions is as yet unresolved. It has been argued that 2D solids lack a long range translational order in the limit $r \to \infty$. One of the consequences of this phenomenon is that the character of the melting transition in two dimensions can be fundamentally different from that of the melting transition in three dimensions. According KTHNY theory two-dimensional solid melts via a two-stage process: first a continuous transition to a hexatic state, followed by a continuous transition to the liquid state [17].

Figure 4(a) shows an isotherm of the lateral pressure as a function of the area, A, in a second set of simulations at constant N, T, A, H. The initial configuration was a monolayer of liquid water taken from the first set and equilibrated for 30 ns at an area of $A = 60.7$ nm^2. The area of the system was then increased or decreased in small incremental steps and simulated for time periods the same as in the first set of simulations. However, in the critical coexistence region the system was equilibrated for 30 ns and an additional 10 ns were run for data collection. For $A > 60.4$ nm^2 the phase is monolayer water while for $A < 54.0$ nm^2 the phase is monolayer ice with the same symmetry and degree of ordering as observed in the simulations at constant lateral pressure. For 54.0 nm$^2 \leq A \leq 60.4$ nm^2 there is a coexistence of the two phases. The vdW loop of the lateral pressure area isotherm [Fig. 4(a)], the sharp linear decrease (resulting from lever rule partitioning) of the energy [Fig. 4(b)], and the phase separation of the two coexisting phases shown in Fig. 4(c) all indicate that the transition is first order.

Experimental studies infer that water stratifies into layers and exhibits an increased oscillatory stress response as the film is reduced to thickness less than four molecular diameters [4]. However, it was also found that the viscosity of water remains comparable to its bulk value even within films down to one or two monolayers thick [18]. It is likely that freezing in confined geometry, which depends on the ability of the molecules to establish inplane interparticle connections, is influenced by competing interfacial interactions.

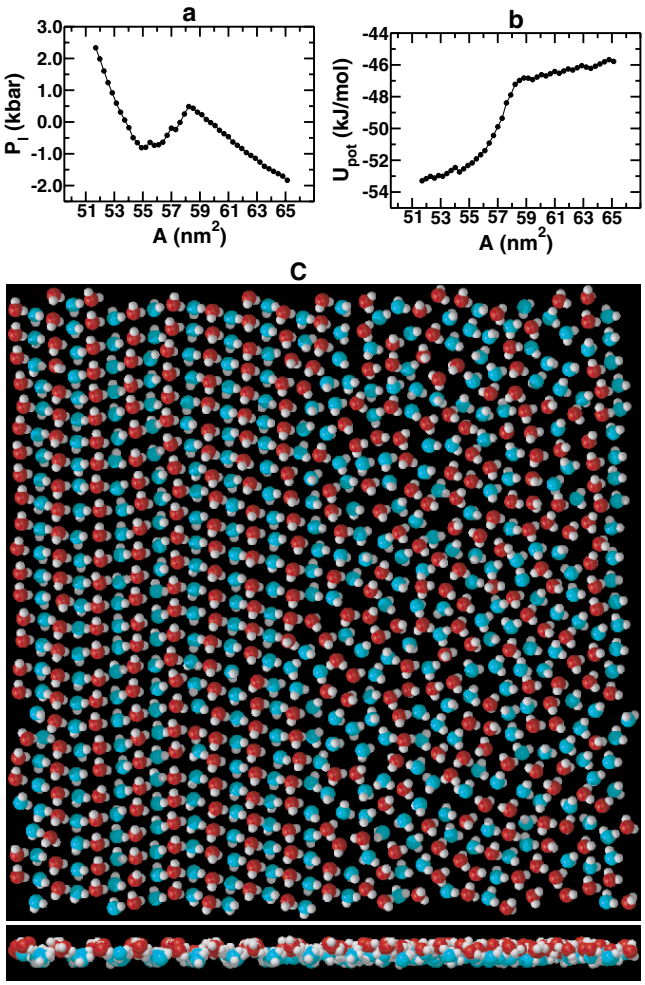

FIG. 4 (color). Simulations at constant number of particles, N, area, A, plate separation, $H = 0.50$ nm, and temperature, $T = 300$ K. Isotherms of (a) the lateral pressure, and (b) the potential energy, as a function of the area. (c) Inplane and out-of-plane views showing the coexistence between water monolayer and ice monolayer obtained at $A = 57.0$ nm^2. Color scheme as in Fig. 3.

The ice monolayer has an inplane rhombic symmetry with respect to the positions of the oxygen atoms. The out-of-plane positions correspond to a linear buckled phase. Experiments with mercury/water/mercury tunnel junctions [5] show that the physical properties of thin film water can vary dramatically (by a few orders of magnitude) and change nonmonotonically with small changes in film thickness, suggesting a change in the film structure. Although these experimental studies were conducted at a $T = 265$ K, we believe the origin of this behavior is due to confinement induced freezing and melting as predicted by the simulations. In addition, the discontinuous transition observed indicates that the KTHNY scenario is preempted by a first-order transition similar to that found in three dimensions. The buckled phase that we find for the ice monolayer was observed before only for (spherical) colloidal particles. The theories that have been proposed to account for such transitions are based on a hard sphere description and have lead to the conclusion that buckling transitions are entropy induced [12]. Our results show that for water this is not the case and that buckling transitions can also be enthalpically driven.

We thank Dr. Uri Raviv for stimulating discussions.

*Corresponding author.
Email address: R.Zangi@chem.rug.nl

[1] B. Kamb, in *Physics and Chemistry of Ice*, edited by E. Whalley, S. J. Jones, and L. W. Gold (Royal Society of Canada, Ottawa, 1973), pp. 28–41.
[2] J. N. Israelachvili, P. M. McGuiggan, and A. M. Homola, Science **240**, 189 (1988).
[3] J. Klein and E. Kumacheva, Science **269**, 816 (1995).
[4] M. Antognozzi, A. D. L. Humphris, and M. J. Miles, Appl. Phys. Lett. **78**, 300 (2001).
[5] J. D. Porter and A. S. Zinn-Warner, Phys. Rev. Lett. **73**, 2879 (1994).
[6] E. Lindahl, B. Hess, and D. van der Spoel, J. Mol. Model. **7**, 306 (2001).
[7] M. W. Mahoney and W. L. Jorgensen, J. Chem. Phys. **112**, 8910 (2000).
[8] R. Zangi and A. E. Mark, J. Chem. Phys. **119**, 1694 (2003).
[9] M. Yamada, S. Mossa, H. E. Stanley, and F. Sciortino, Phys. Rev. Lett. **88**, 195701 (2002).
[10] T. Ogawa, J. Phys. Soc. Jpn. Suppl. **52**, 167 (1983).
[11] D. H. van Winkle and C. A. Murray, Phys. Rev. A **34**, 562 (1986).
[12] M. Schmidt and H. Löwen, Phys. Rev. E **55**, 7228 (1997).
[13] R. Zangi and S. A. Rice, Phys. Rev. E **58**, 7529 (1998).
[14] S. Neser, C. Bechinger, P. Leiderer, and T. Palberg, Phys. Rev. Lett. **79**, 2348 (1997).
[15] R. Zangi and S. A. Rice, Phys. Rev. E **61**, 660 (2000).
[16] L. Pauling, J. Am. Chem. Soc. **57**, 2680 (1935).
[17] K. J. Strandburg, Rev. Mod. Phys. **60**, 161 (1988).
[18] U. Raviv, P. Laurat, and J. Klein, Nature (London) **413**, 51 (2001).